



**HAL**  
open science

# Corneal Changes in Acanthamoeba Keratitis at Various Levels of Severity: An In Vivo Confocal Microscopic Study

Zhenyu Wei, Kai Cao, Leying Wang, Christophe Baudouin, Antoine Labbé, Qingfeng Liang

► **To cite this version:**

Zhenyu Wei, Kai Cao, Leying Wang, Christophe Baudouin, Antoine Labbé, et al.. Corneal Changes in Acanthamoeba Keratitis at Various Levels of Severity: An In Vivo Confocal Microscopic Study. *Translational vision science & technology*, 2021, 10 (7), pp.10. 10.1167/tvst.10.7.10 . hal-03258534

**HAL Id: hal-03258534**

**<https://hal.sorbonne-universite.fr/hal-03258534v1>**

Submitted on 11 Jun 2021

**HAL** is a multi-disciplinary open access archive for the deposit and dissemination of scientific research documents, whether they are published or not. The documents may come from teaching and research institutions in France or abroad, or from public or private research centers.

L'archive ouverte pluridisciplinaire **HAL**, est destinée au dépôt et à la diffusion de documents scientifiques de niveau recherche, publiés ou non, émanant des établissements d'enseignement et de recherche français ou étrangers, des laboratoires publics ou privés.

# Corneal Changes in *Acanthamoeba* Keratitis at Various Levels of Severity: An In Vivo Confocal Microscopic Study

Zhenyu Wei<sup>1</sup>, Kai Cao<sup>1</sup>, Leying Wang<sup>1</sup>, Christophe Baudouin<sup>1-3</sup>, Antoine Labbé<sup>1-3</sup>, and Qingfeng Liang<sup>1</sup>

<sup>1</sup> Beijing Institute of Ophthalmology, Beijing Tongren Eye Center, Beijing Tongren Hospital, Capital Medical University, Beijing Key Laboratory of Ophthalmology and Visual Sciences, Beijing, China

<sup>2</sup> Quinze-Vingts National Ophthalmology Hospital, IHU FOReSIGHT, Paris and Versailles Saint-Quentin-en-Yvelines University, Versailles, France

<sup>3</sup> Institut de la Vision, IHU FOReSIGHT, Sorbonne Université, INSERM, CNRS, Paris, France

**Correspondence:** Qingfeng Liang, Beijing Institute of Ophthalmology, Beijing Tongren Eye Center, Beijing Tongren Hospital, Capital Medical University, Beijing Key Laboratory of Ophthalmology and Visual Sciences, Beijing 100005, China.  
e-mail: [liangqingfeng@ccmu.edu.cn](mailto:liangqingfeng@ccmu.edu.cn)

**Received:** March 23, 2020

**Accepted:** April 25, 2021

**Published:** June 10, 2021

**Keywords:** in vivo confocal microscopy; *Acanthamoeba* keratitis; cyst; dendritic cell

**Citation:** Wei Z, Cao K, Wang L, Baudouin C, Labbé A, Liang Q. Corneal changes in *Acanthamoeba* keratitis at various levels of severity: An in vivo confocal microscopic study. *Transl Vis Sci Technol.* 2021;10(7):10, <https://doi.org/10.1167/tvst.10.7.10>

**Purpose:** To investigate the relationship between *Acanthamoeba* cysts and inflammatory cells in *Acanthamoeba* keratitis (AK) by in vivo confocal microscopy (IVCM).

**Methods:** A case-control study included 30 patients with AK and 20 normal controls. The severity of the AK was divided into mild, moderate, and severe. The central cornea and four standard quadrants of the peripheral cornea were imaged by IVCM. The cyst infiltration and dendritic cell (DC) density and maturity (size, length, field, and number of dendrites) were quantified. The relationship between clinical severity, cyst density, and DC alterations was characterized by Spearman correlation analysis.

**Results:** The maximum cyst density in the mild, moderate, and severe groups was 31.3 cysts/mm<sup>2</sup> (17.2–32.8), 62.5 cysts/mm<sup>2</sup> (59.3–103.1), and 162.5 cysts/mm<sup>2</sup> (65.6–215.6), respectively. Compared to normal participants, a significant increase in the mean corneal DC density was detected in patients with AK (290.2 ± 97.0 vs. 25.3 ± 8.3 cells/mm<sup>2</sup>;  $P < 0.001$ ). Patients with AK presented an increase in median DC size (178.3 vs. 63.6 μm<sup>2</sup>/cell,  $P < 0.001$ ), median DC field (518.1 vs. 256.6 μm<sup>2</sup>/cell,  $P = 0.008$ ), and median DC dendrite length (42.3 vs. 14.7 μm/cell,  $P < 0.001$ ). Increased AK severity was correlated with an increase in cyst density, DC size, and dendrite length (all  $P < 0.05$ ). An increase in cyst density was significantly correlated with an increase in DC density ( $\beta = 0.484$ ,  $P = 0.026$ ) and DC size ( $\beta = 0.557$ ,  $P = 0.009$ ).

**Conclusions:** Cyst density and depth of infiltration as well as maturity of the surrounding DC increased significantly with the severity of AK.

**Translational Relevance:** Quantitative analysis of cyst density and DC maturity may provide a new method of evaluating the severity of AK.

## Introduction

*Acanthamoeba* keratitis (AK) is a rare but potentially blinding corneal infection caused by the opportunistic free-living protozoan, *Acanthamoeba*. Contact lens (CL) wear is one of most important risk factors for AK. With the increasing use of contact lenses around the world, the incidence of AK is obviously rising.<sup>1,2</sup> Carnt et al.<sup>3</sup> reported 36 to 65 AK cases per year in the United Kingdom from 2010 to 2017, representing a three to five times increase in incidence compared to

2004 to 2009 (15–23 cases per year). The recent development of orthokeratology, which employs overnight rigid contact lens wear for correction of refractive errors, is also showing a high risk of AK.<sup>4</sup>

Eliminating the infective microorganism and suppressing the inflammatory response remain the main treatment for AK. While the pathogenic trophozoites infiltrate the corneal stroma, inflammatory cells also accumulate within the ocular surface tissues. Kremer et al.<sup>5</sup> detected chronic stromal inflammation, with macrophages and polymorphonuclear leukocytes, in patients with AK. Sohn et al.<sup>6</sup> found an increase

in mRNA expression of interleukin (IL)-1 $\alpha$ , IL-6, and IL-8 in in vitro co-culture between trophozoites or cysts and corneal epithelial cells. Similarly, as persistent inflammatory responses are present in some cases of AK, systemic or local steroids, or immunosuppressive agents, have occasionally been used, but no clear consensus has been defined on their use.<sup>7-9</sup> Consequently, it is important to investigate the mechanisms of inflammation in AK as well as the relationship between *Acanthamoeba* and the corneal inflammatory response.

In vivo confocal microscopy (IVCM) has been used as a noninvasive imaging technique for the analysis of normal and pathologic corneal microstructures. Huang et al.<sup>10</sup> quantified the density and depth of *Acanthamoeba* cysts in the cornea in various stages of AK and found that invasion of *Acanthamoeba* cysts into Bowman's layer might be a useful predictor of a persistent clinical course. Cruzat et al.<sup>7</sup> used IVCM to reveal the density of and morphologic changes in central epithelial dendritic cells (DCs) in infectious keratitis. Using these methods of evaluation, the purpose of the present study was to quantitatively analyze the relationship between *Acanthamoeba* cysts and inflammatory cells in AK.

## Methods

### Participants

This study was conducted at the Beijing Institute of Ophthalmology between January 2017 and January 2019 with the approval of the Medical Ethics Committee of Beijing Tongren Hospital (TRECKY2015-KY09), Beijing, China. In this case-control study, 30 patients diagnosed with AK by clinical manifestations and laboratory tests (positive corneal scraping or cultures for *Acanthamoeba*) and 20 age- and gender-matched normal participants were enrolled. All participants were informed of the goals of the study, and their consent was obtained in accordance with the Declaration of Helsinki. Patients with a history of any other infectious keratitis, ocular inflammation, ocular trauma, or eye surgery within the previous 6 months were excluded.

### Clinical Evaluation

Patient information was recorded using a standard protocol that included demographics, duration of symptoms, predisposing factors, initial diagnosis and treatments, time to AK diagnosis, clinical features, associated ocular conditions, and systemic diseases.

Risk factors for AK were recorded, including contact lenses wear, ocular trauma, or exposure to potentially contaminated water.

After measurement of visual acuity, all patients were examined by slit-lamp biomicroscopy. The size of the corneal ulcer and stromal infiltration were measured on corneal photographs with ImageJ software (National Institutes of Health, Bethesda, MD, USA) and recorded in millimeters. The depth of ulcer and stromal infiltration were assessed at the slit lamp, recording the depth ratio of infiltration (or ulcer)/total cornea thickness. The presence or absence of hypopyon was recorded and the height measured in millimeters. Based on the severity grading system for infectious corneal ulcers,<sup>8,9</sup> patients with AK were graded as mild (corneal ulcer diameter <2 mm, ulcer depth <20%, and infiltration depth <20%), moderate (corneal ulcer diameter 2–5 mm and/or ulcer depth 20%–50% and/or infiltration depth 20%–50%), and severe (corneal ulcer diameter >5 mm or ulcer depth >50% or infiltration depth >50%). The grouped results were graded with priority given to the most serious criteria. Laboratory investigations for AK included corneal scrapings, optical microscopic observation after Giemsa staining, and cultures on nonnutrient agar plates overlaid with *Escherichia coli*, performed in the Department of Ocular Microbiology at the Beijing Institute of Ophthalmology. All included patients had a positive stain or culture for AK.

### In Vivo Confocal Microscopy Examination

For all participants, IVCM images were obtained using the new Rostock Cornea Module of the Heidelberg Retina Tomograph (HRT III) (Heidelberg Engineering GmbH, Heidelberg, Germany). The laser source employed in the HRT III/RCM is a diode laser with a wavelength of 670 nm. Images are 384 × 384 pixels, covering an area of 400 × 400  $\mu$ m, with transversal optical resolution of approximately 1  $\mu$ m/pixel and an acquisition time of 0.024 seconds, according to Heidelberg Engineering. Just prior to the examination, a drop of topical anesthetic (proparacaine hydrochloride, 0.5%) was instilled into the inferior conjunctival fornix. The position of the eye was adjusted and monitored by means of a live image from a color CCD camera (640 × 480 pixels, RGB, 15 frames/s). IVCM was performed in section mode by two experienced ophthalmologists (ZW and LW) masked for patient clinical data. Images of the central cornea and four standard quadrants of the peripheral cornea (superior, temporal, inferior, and nasal) were obtained. Images of the corneal ulcer and the surrounding cornea were also acquired. Fifty high-quality images from the

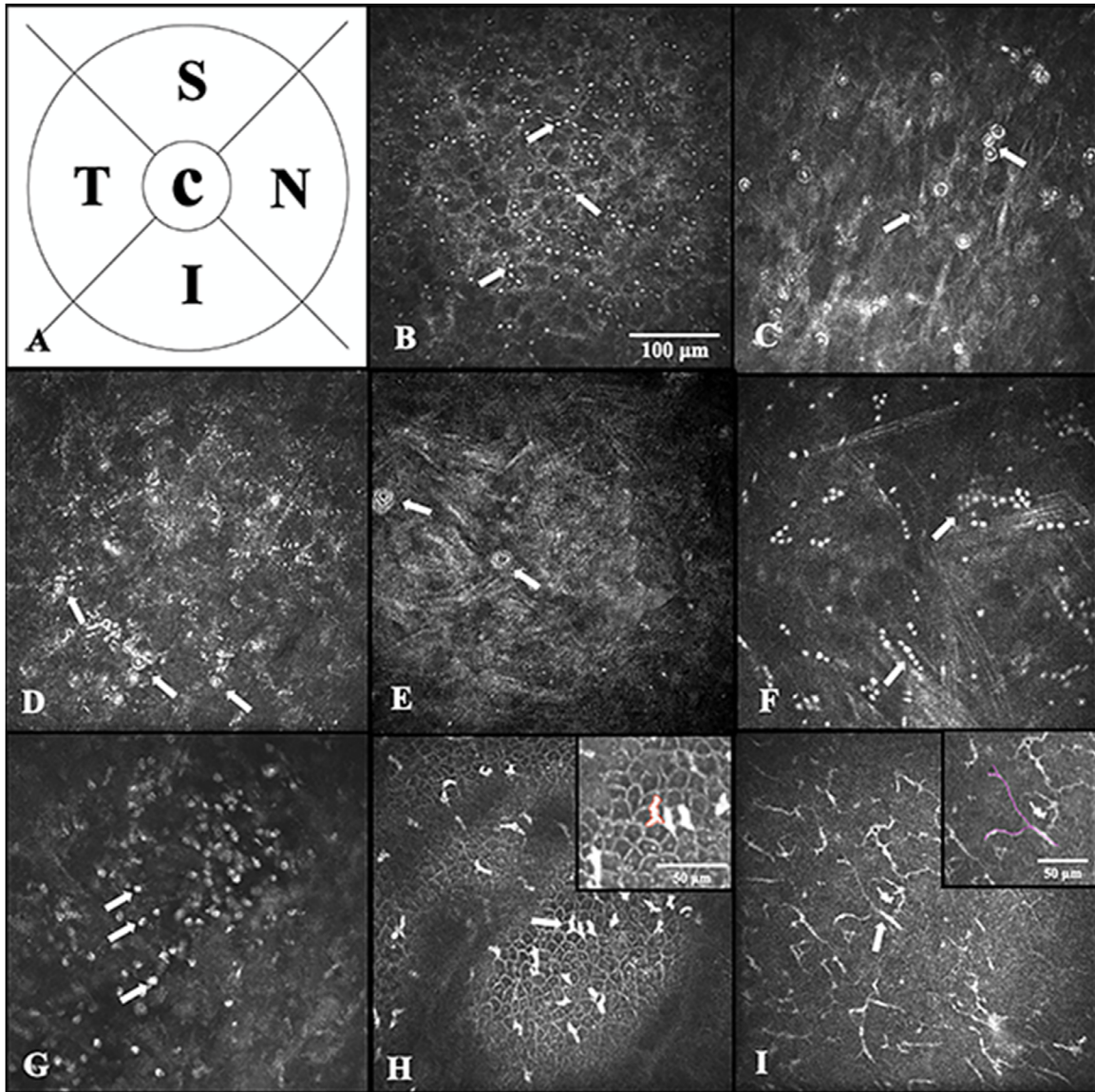


**Figure 1.** IVCM images ( $400 \times 400 \mu\text{m}$ ) of *Acanthamoeba* cysts and inflammatory cells. (A) Schematic view of the five corneal areas: central cornea (C), superior (S), inferior (I), nasal (N), and temporal (T) peripheral cornea. (B–E) *Acanthamoeba* cyst subtypes: (B) bright spot, (C) signet ring appearance, and (D, E) thick double-walled structure. (F) Linear arrangement of *Acanthamoeba* cysts. (G–I) Inflammatory cell subtypes: (G) round cell, (H) dendritic cells with small processes, and (I) dendritic cells with long processes.

epithelium to the endothelium were acquired in each area, representing approximately 10 images per layer.

### Image Analysis

Confocal images were anonymized and analyzed separately in a masked manner by two ophthalmologists (KC and QL). Interobserver differences were calculated, and when a discrepancy exceeded 10%, a third ophthalmologist analyzed the images, and the results of the three independent evaluations

were averaged. A protocol to identify *Acanthamoeba* cysts, inflammatory round cells, and inflammatory DCs on IVCM was established according to previous studies.<sup>7,11–15</sup> Typical cysts were defined as highly reflective structures (about  $10\text{--}40 \mu\text{m}$ <sup>11,12</sup>), with a bright spot, signet ring appearance, or double-walled structure (Figs. 1B–F). Inflammatory round cells were described as small ( $<10 \mu\text{m}$ <sup>13</sup>), hyperreflective, oval-shaped cells with no visible fibrils, ring shape, or double-walled structure (Fig. 1G). DCs consistently manifest a bright dendritiform structure along with



the cell body (Figs. 1H, 1I). Two types of DCs were quantified: DCs with small processes and DCs with long processes.<sup>14</sup>

### Mean Density of *Acanthamoeba* Cysts

Using the method by Huang et al.,<sup>10</sup> the cyst density and the depth of infiltration were evaluated with the Cell Count Software on the HRT3/RCM. From the epithelial layer to the endothelial layer in the central area of the AK ulcer, three images with maximum cyst density (cysts per square millimeter) at a depth of every 50  $\mu\text{m}$  were selected, and the mean value was taken as the mean cyst density at this depth.

### Mean Density and Size of Dendritic Cells

According to the same protocol mentioned above, 15 images with maximum DC density in the five detected areas (three images in each area) were selected from the epithelial layer to Bowman's layer.<sup>15</sup> The mean value of these 15 images was taken as the mean corneal DC density. Only the DCs with clear cell bodies were counted (Supplementary Fig. S1). Patients without the epithelial layer in the center of the cornea were excluded from analysis. Using these images of DC, DC size (the size of the hyperreflective DC structure) and number of dendrites per DC were measured by ImageJ software (National Institutes of Health) (Fig. 1H). To measure the total DC length, all dendrites were traced from the cell body to the end of the highly reflective dendrites using NeuronJ software (National Institutes of Health, Bethesda, MD, USA) (Fig. 1I). The lengths of all the dendrites of each DC were added to yield the total DC length. DC field corresponded to the area connecting the dendrite tips around each cell.<sup>16</sup>

### Statistical Analysis

Statistical analysis was performed with R software (R Development Core Team, Vienna, Austria). The significance level was 0.05, but for pairwise comparison among multiple subgroups (such as mild, moderate, and severe AK), the significance level was adjusted by the Bonferroni method. The Kolmogorov–Smirnov test (Supplementary Table S1) was used for testing the normality of each variable. These parameters were compared between the controls and patients with AK in the various stages using the  $\chi^2$  test (for categorical data) and Wilcoxon rank sum test (for continuous data). The association between clinical parameters and IVCN results was characterized by a linear mixed-effects model. For better presentation of the data distribution, a box plot, bar plot, and matrix scatterplot were presented. All of the above measurements (clinical evaluation and IVCN measurement) were performed

by two independent, masked, experienced observers. Interobserver differences were calculated to assess the interoperator variation.

## Results

A total of 50 eyes were included in this study: 30 eyes of 30 patients with AK and 20 eyes of 20 control participants. The median age was 46.0 years (interquartile range [IQR], 21.0–52.8) in the AK group and 50.0 years (IQR, 47.0–53.0) in the control group. There was no significant difference in age ( $P = 0.279$ ) or gender ( $P = 0.928$ ) between these two groups.

### Clinical Manifestations

Of the 30 patients with AK, 4 cases (13.3%) had a history of contact lens wear prior to the onset of symptoms. Five cases (16.7%) had a history of ocular injury (agricultural, dust, or metal injury), and 3 cases (10%) had a history of tap water exposure. The average time to AK diagnosis was  $53.2 \pm 39.4$  days (ranging from 5 days to 6 months). Of the 30 patients, 21 (70%) were treated initially with topical antibiotics and 18 (60%) for herpes simplex keratitis with topical antiviral medication. Before being diagnosed with AK, 2 patients (6.7%) had been given topical corticosteroids, and their lesions presented in the moderate stage. At the initial visit, the decimal visual acuity of 14 cases (46.7%) was less than 0.02, 9 cases (30.0%) were between 0.02 and 0.3, and 7 cases (23.3%) were greater than 0.3. Thirty (100%) cases had a central corneal infiltration or ulcer, 24 (80%) had peripheral stromal infiltrates, and 6 (18%) had total corneal involvement. The median size of the corneal ulcers was 6.5 mm (IQR, 3.3–8.0), and the mean size of the infiltrates was 8.0 mm (IQR, 6.3–9.0). The median depth of ulcer/infiltrate was 40% (IQR, 30%–60%) of the total cornea thickness (Table 1).

According to the ulcer size and infiltration depth, AK was divided into mild (8 cases), moderate (7 cases), and severe (15 cases). In mild cases, epithelial infiltrates were seen as pseudodendritic epithelial lesions (3 cases), epithelial ridges (2 cases), or defects (4 cases). Few ring infiltrates or anterior uveitis were observed at this stage. In moderate and severe cases, stromal involvement, including ring infiltrate (5 cases) and ulcer (13 cases), endothelial plaques (5 cases), and corneal thinning or hypopyon (4 cases), was common (Fig. 2). Visual acuity was greater than 0.3 in 87.5% of mild cases (7/8 cases) and less than 0.02 in 93.3% of severe cases (14/15 cases). All moderate cases, one mild case,

**Table 1.** Demographics and Clinical Characteristics of Patients and Normal Controls

Parameter	Patients	Normal Controls
Gender, <i>n</i> (%)		
Male	18 (60.0)	12 (60.0)
Female	12 (40.0)	8 (40.0)
Age, y	46.0 (21.0–52.8)	50.0 (47.0–53.0)
Duration, d	55.0 (27.8–60.0)	
Risk factor, <i>n</i> (%)		
Contact lens use	4 (13.3)	
Ocular surface injury	5 (16.7)	
Agricultural	3 (10)	
Dust	1 (3.3)	
Metal	1 (3.3)	
Tap water exposure	3 (10)	
Unknown	18 (60)	
Visual acuity (decimal), <i>n</i> (%)		
>0.3	7 (23.3)	
0.02–0.3	9 (30.0)	
<0.02	14 (46.7)	
Ulcer size, mm	6.5 (3.3–8.0)	
Infiltration size, mm	8.0 (6.3–9.0)	
Ulcer/infiltration depth, %	40 (30–60)	
Scraping (+/–), <i>n</i>	19/11	
Culture (+/–), <i>n</i>	21/9	
Severity of AK, <i>n</i> (%)		
Mild	8 (26.7)	
Moderate	7 (23.3)	
Severe	15 (50.0)	

and one severe case had visual acuity between 0.02 and 0.3.

Giemsa staining of the scraping was positive in 19 cases (63.3%), with blue-purple cyst walls (Fig. 2, third line) and/or trophozoites. Twenty-one of the 30 AK cases (70%) were culture positive on nonnutrient agar plates overlaid with *Escherichia coli*.

### In Vivo Confocal Microscopy of *Acanthamoeba* Cysts

*Acanthamoeba* cysts were detected in all AK cases by IVCN examination. Cysts appeared as highly reflective round to oval structures with ring or double-wall characteristics. The cysts were arranged as single randomly located spots or in chains (Fig. 2). The density and depth of *Acanthamoeba* infiltration was able to be evaluated in all AK cases. Trophozoites were detected in only two patients by IVCN. To ensure the accuracy of the investigation, an intraclass correlation

coefficient (ICC) between the two observers was evaluated. The ICCs for counting cysts and DCs were 0.989 and 0.963, respectively, and the 95% confidence intervals (CIs) for observer bias were 0.973 to 0.996 for cyst calculation and 0.909 to 0.985 for calculations of DC parameters.

As the scanning depth increased, the mean cyst densities decreased ( $P = 0.002$ ). The highest density of cysts was located at 0 to 100  $\mu\text{m}$  (Fig. 3). In this superficial layer (less than 100  $\mu\text{m}$  depth), the medians of the maximum cyst densities were 31.3 cysts/ $\text{mm}^2$  (IQR, 17.2–32.8), 62.5 cysts/ $\text{mm}^2$  (IQR, 59.3–103.1), and 162.5 cysts/ $\text{mm}^2$  (IQR, 65.6–215.6) ( $P = 0.031$ ) in the mild, moderate, and severe groups, respectively. The cyst density in the severe group was significantly higher than that of the mild group ( $P = 0.009$ ) or the moderate group ( $P = 0.047$ ). There was no significant difference between the mild and moderate groups ( $P = 0.837$ ). The cyst densities in the AK patients' peripheral corneas are provided in Supplementary Table S2.

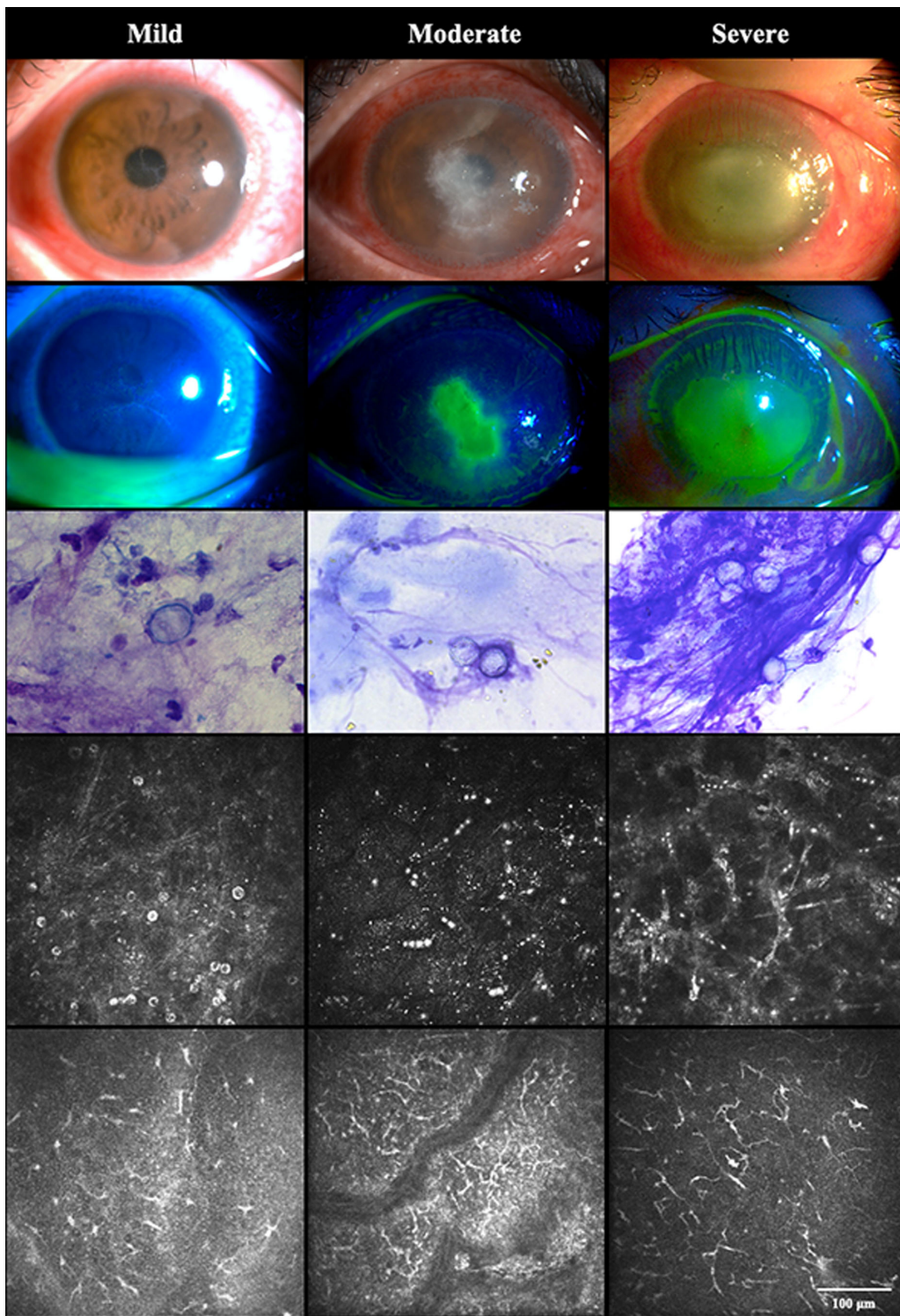


**Figure 2.** Representative examples of slit-lamp appearance, scraping cytology, and IVCM scanning in patients with AK in mild, moderate, and severe stages. Slit-lamp photos (first line) and fluorescein staining patterns (second line) are shown. Scraping cytology images of the corneal lesion (Giemsa staining, 1000 $\times$ , third line) and IVCM scanning (fourth line) in patients with AK are shown (IVCM image, 400  $\times$  400  $\mu$ m).



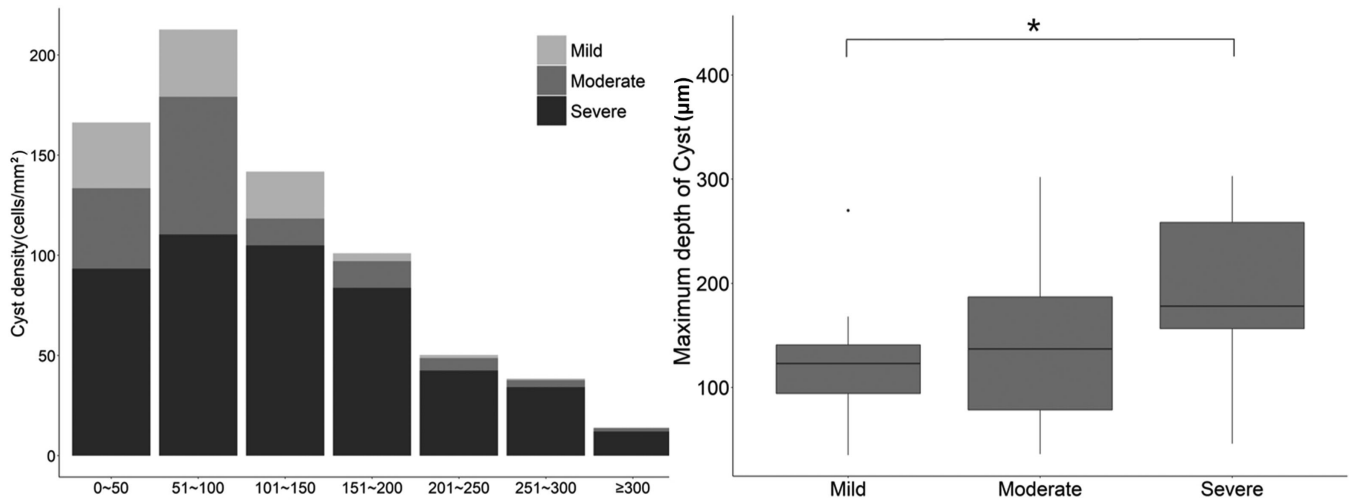


**Figure 3.** The density of *Acanthamoeba* cysts varied according to the depth of the IVC examination (left). The maximum cyst infiltration depth in patients with AK with various degrees of severity (right). \*Statistically significant difference ( $P < 0.05$ ).

**Table 2.** Quantitative Analysis of DCs for Patients with AK and Control Group

Parameters	Patients	Normal Controls	P Value
Gender, n (%)			
Male	18 (60.0)	12 (60.0)	0.928
Female	12 (40.0)	8 (40.0)	
Age, y	46.0 (21.0–52.8)	50.0 (47.0–53.0)	0.279
DC density, cells/mm <sup>2</sup>			
Center <sup>a</sup>	213.6 ± 33.2	20.8 ± 5.8	<0.001
Periphery	331.4 ± 61.0	34.4 ± 2.5	<0.001
DC size, μm <sup>2</sup>	178.3 (140.0–252.1)	63.6 (47.9–69.8)	<0.001
DC length, μm	42.3 (30.9–61.5)	14.7 (11.5–18.5)	<0.001
DC field, μm <sup>2</sup>	518.1 (293.0–635.8)	256.6 (133.7–321.2)	0.008
Number of DC dendrites	2.0 (1.7–2.2)	2.5 (2.0–2.9)	0.068

<sup>a</sup>Only 21 cases (8 mild patients, 7 moderate patients, 6 severe patients) with epithelium were included into DCs' quantitative analysis.

The median of the maximum cyst infiltration depth was 123 μm (IQR, 94.3–141.0), 137 μm (IQR, 78.5–187.0), and 178 μm (IQR, 156.5–258.5) in the mild, moderate, and severe groups, respectively. The maximum cyst infiltration depth increased with the severity of disease ( $P = 0.043$ ).

### In Vivo Confocal Microscopy of Dendritic Cells

Dendritic cells were consistently located within the sub-basal corneal layer, near the nerve plexus. There were only 21 cases (8 mild patients, 7 moderate patients, 6 severe patients) with epithelium included into DCs' quantitative analysis. Quantitative analysis of DC density, DC size, and number of DC dendrites

in the central cornea and the four quadrants of the peripheral cornea for patients with AK and normal controls are shown in Table 2. Compared to normal controls ( $25.3 \pm 8.3$  cells/mm<sup>2</sup>), a higher DC density was detected in patients with AK ( $290.2 \pm 97.0$ ,  $P < 0.001$ ). According to subgroup analysis, DC density increased with severity, but there was no significant difference in DC density between the AK subgroups (all  $P > 0.05$ ; Fig. 4).

Given the nonuniform distribution of DCs between the central and peripheral cornea, the peripheral and central corneal changes in DCs were analyzed independently. In the central cornea, the DC density was  $213.6 \pm 33.2$  cells/mm<sup>2</sup> in patients with AK and  $20.8 \pm 5.8$  cells/mm<sup>2</sup> in normal controls ( $P < 0.001$ ). In the peripheral cornea, compared to normal controls



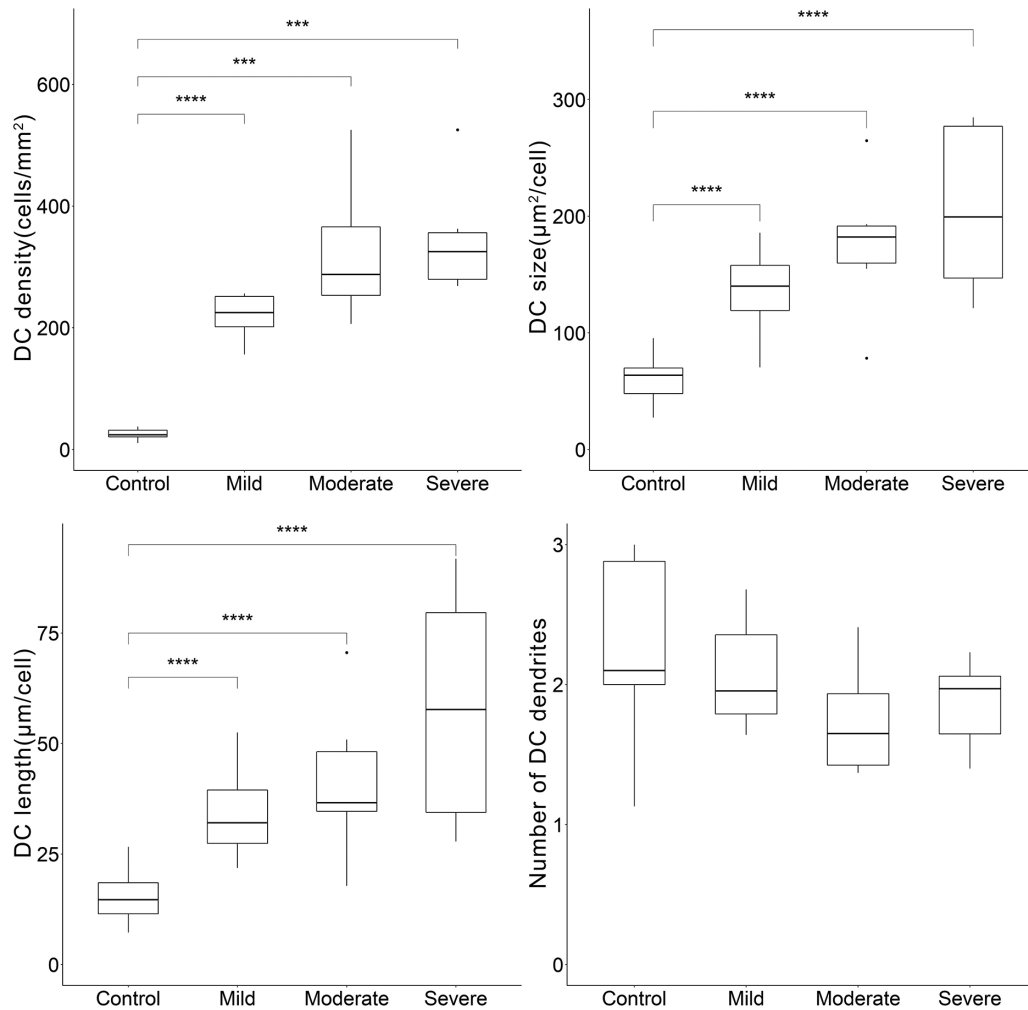


**Figure 4.** Distribution of DC density, size, length, and the number of dendrites in the AK group and control group. \*Statistically significant difference ( $P < 0.05$ ).

( $34.4 \pm 2.5$  cells/mm<sup>2</sup>), a higher DC density was detected in patients with AK ( $331.36 \pm 61.0$  cells/mm<sup>2</sup>,  $P < 0.001$ ).

IHCM revealed DC morphologic changes in the AK group. While a few small DCs (presumably immature) were present in normal corneas, patients with AK presented an obvious increase in both median DC size (178.3 vs. 63.6 μm<sup>2</sup>/cell,  $P < 0.001$ ), DC field (518.1 vs. 256.6 μm<sup>2</sup>/cell,  $P = 0.008$ ), and median DC dendrite length (42.3 vs. 14.7 μm/cell,  $P < 0.001$ ), presumably characteristics of a more mature phenotype. With the increasing of AK severity, the DC size and dendritic length also increased (both  $P < 0.001$ ). The median number of DC dendrites was not statistically different between the AK and control groups (2.0 vs. 2.5,  $P = 0.068$ ) (Table 2). Similarly, there was no statistically significant difference between each AK subgroup and the control group (all  $P > 0.05$ ; Fig. 4).

### Correlation Between Cyst Density and DC Alterations

In the AK group, ulcer size was positively associated with cyst density ( $\beta = 0.638$ ;  $P = 0.002$ ), DC density ( $\beta = 0.583$ ;  $P = 0.006$ ), and DC size ( $\beta = 0.463$ ;  $P = 0.035$ ). Increasing cyst density was significantly associated with increasing DC density ( $\beta = 0.484$ ;  $P = 0.026$ ) and DC size ( $\beta = 0.558$ ;  $P = 0.009$ ). In addition, DC density was positively associated with DC size ( $\beta = 0.775$ ;  $P < 0.001$ ) and DC length ( $\beta = 0.778$ ;  $P < 0.001$ ). We found no significant association between ulcer size and DC length ( $\beta = 0.268$ ;  $P = 0.240$ ) or between cyst density and DC length ( $\beta = 0.376$ ;  $P = 0.092$ ) (Fig. 5). The number of DC dendrites showed no significant association with any clinical or imaging parameters (all  $P > 0.05$ ).

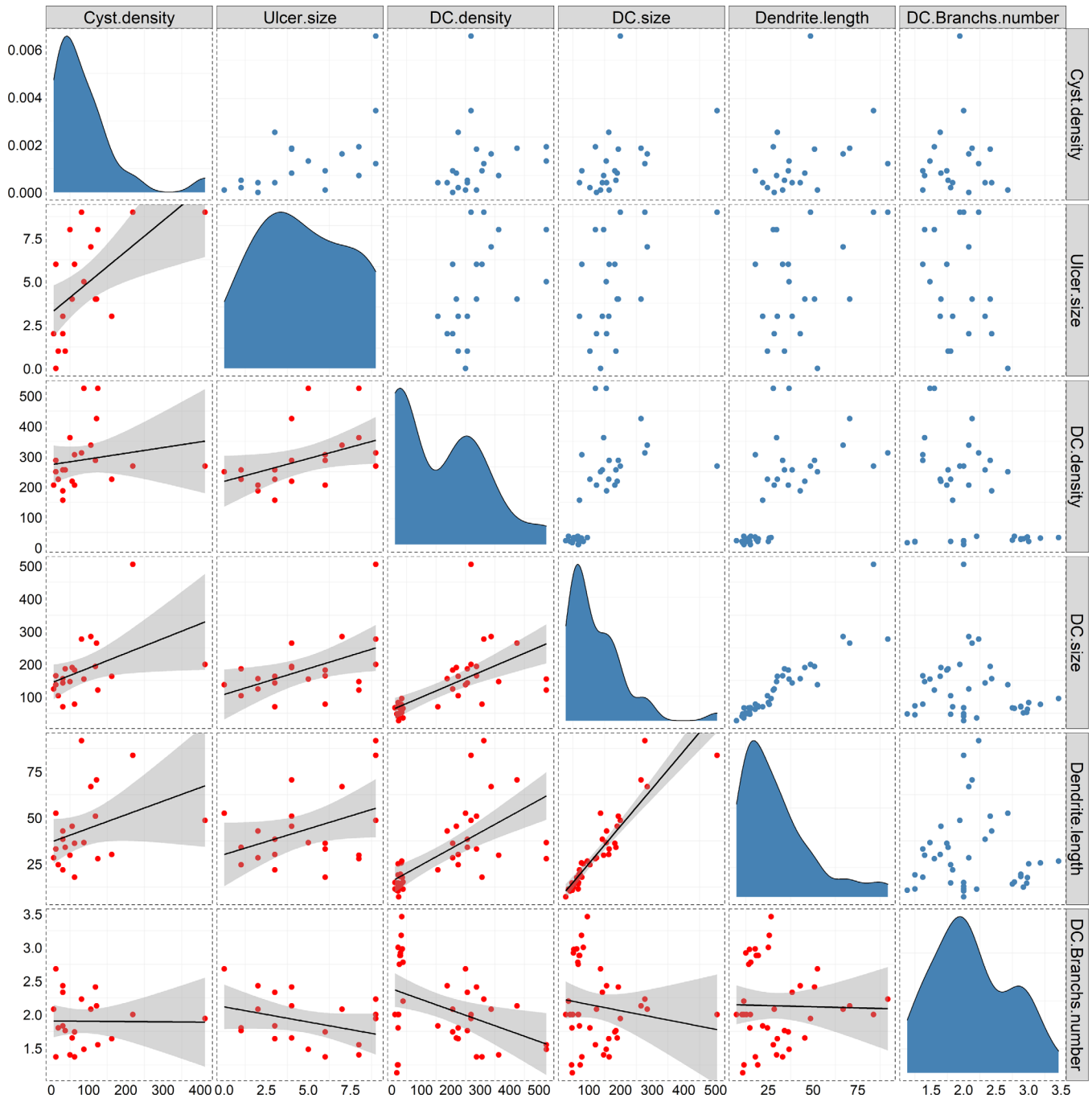


Figure 5. Scatterplot of correlation between cyst density and dendritic cell alterations. \*Statistically significant correlation coefficients.

## Discussion

*Acanthamoeba* keratitis is a sight-threatening corneal infection. The relationship between pathogenic strains of *Acanthamoeba* and infiltration of inflammatory cells might play a critical role in the course of AK. The timely use of noninvasive IVCM may provide a novel evaluation of cyst morphology and distribu-

tion as well as density, distribution, and morphologic changes of immune cells (including DCs) in AK.<sup>17</sup> To our knowledge, this is the first study to analyze cyst infiltration, epithelial DCs changes, and their potential correlations in AK. We found that *Acanthamoeba* cysts were observed mainly in the epithelium and anterior stroma. Increasing cyst density was also significantly correlated with increasing DC size and dendrite length in patients with AK.

Previous studies have suggested that IVCM might be an interesting technique for evaluation of the distribution and depth of cysts in AK cases.<sup>17,18</sup> Wang et al.<sup>18</sup> used IVCM to monitor AK progression by mean cyst density. In the present study, *Acanthamoeba* cysts were distributed mainly in the anterior 100  $\mu\text{m}$  of the corneal epithelium and anterior stroma. IVCM detection of AK cysts in infectious keratitis remains a challenge for ophthalmologist. Therefore, with the objective of improving the positive detection rate, IVCM examination for *Acanthamoeba* cysts should be concentrated within a depth of 50 to 100  $\mu\text{m}$ . The mean cyst density within the central cornea was  $106.5 \pm 98.9$  cysts/ $\text{mm}^2$ , which was very consistent with the results of the study by Wang et al.<sup>18</sup> ( $99 \pm 64.9$  cysts/ $\text{mm}^2$ ). Although Huang et al.<sup>10</sup> reported that the mean cyst density was  $177.9 \pm 99.6$  cysts/ $\text{mm}^2$ , it was higher than the average level in our study but similar to the cyst density in our severe cases ( $162.5 \pm 36.2$  cysts/ $\text{mm}^2$ ). Among their 18 cases, four eyes (19.0%) underwent therapeutic keratoplasty, whereas our patients were controlled with medical treatment. The difference in cyst density might be explained by the difference in AK severity between the two studies, with their cases being more severe. A higher density and deeper infiltration of cysts were associated with a larger size of AK ulcer in the present study. These findings are in accordance with previous IVCM results from Huang et al.,<sup>10</sup> suggesting that these two parameters are associated with the severity of AK.

Some studies have revealed that granulomatous inflammation and the immune response are critical mechanisms in the course of AK.<sup>19–21</sup> Macrophages and polymorphonuclear leukocytes seem to be the predominant cells in the inflammatory infiltrate of AK.<sup>19</sup> In the present study, a significant increase in DC density was shown in patients with AK, especially in the mild and moderate AK subgroups. Compared to controls, a three times increase in DC size and dendrite length was found in AK cases. A similar result was observed by Cruzat et al.,<sup>7</sup> who demonstrated a significant increase in DC density in cases with infectious keratitis compared to controls ( $672.9 \pm 791.5$  vs.  $49.3 \pm 39.6$ ;  $P < 0.0001$ ). In addition, some studies have shown that mature DCs can be recognized by morphologic changes, including numerous long dendrites and increased size.<sup>14,22</sup> Zhivov et al.<sup>14</sup> used IVCM to examine DC distribution in 200 normal corneas of 112 healthy volunteers and found that mature DCs appeared in the peripheral cornea with numerous long dendrites. In the central cornea, DCs often lacked or had only a few small dendrites. Consequently, the size and length of DCs might be used to evaluate the degree of maturity of DCs. In the present study, the size and

dendrite length of DCs increased with increasing AK severity. This suggests that amoebic cysts might induce cell-mediated immunity and an inflammatory response. Cell-derived cytokines and chemokines (tumor necrosis factor  $\alpha$ , IL-1, and macrophage inflammatory protein (MIP)-1 $\alpha$  and MIP- $\beta$ ) can regulate the movement of DCs from the periphery toward the center.<sup>22</sup> In a mouse model, cysts induced a lymphoproliferative response in splenic T cells from mice immunized against *Acanthamoeba* cysts.<sup>23</sup> Although the adaptive immune response cannot kill the cysts, antiparasite antibodies or complement induced by cysts help to stimulate a neutrophil-mediated inflammatory response. Therefore, integration of both the innate and adaptive immune response is very important to remove amoeba from the cornea. Unfortunately, it is not possible to distinguish the detailed characteristics of round cells such as neutrophils, basophils, or eosinophils by IVCM. DC density and maturation increased with the size of the corneal ulcer in the mild and moderate stages of AK. However, in the severe subgroup, while DC exhibited a highly mature stage, the DC density was lower. As more cysts transform into trophozoites in the severe stage of AK, neutrophil inflammation might downregulate any subsequent lymphoproliferative response to cyst antigens.<sup>5</sup> Clarke and Niederkorn<sup>20</sup> suggested that cell-mediated immunity may not be very effective in controlling severe AK. Consequently, at this stage, corticosteroid use may increase tissue damage and induce or worsen chronic AK.<sup>24</sup> In all AK cases, ulcer size was positively correlated with cyst density and DC density, emphasizing the link between inflammation and infection in AK. Although we did not find a significant correlation between cyst density and DC density, cyst density was positively correlated with DC size and DC length. Using IVCM, it might be possible to monitor inflammatory conditions by detecting DC maturation. Although not widely accepted, anti-inflammatory and immunosuppressive treatments have been reported in some studies on AK management.<sup>25–27</sup> Based on the present results, it would be interesting to evaluate in vivo corneal inflammatory conditions by IVCM.

This study has several limitations. First, in severe AK cases with large epithelial defects or ulcers, the quantitative analysis of dendritic cells could be difficult. In our study, 15 cases of severe AK had a whole corneal ulcer and lacked epithelial and Bowman's layers. This might explain the result of a decrease in DC density in patients with severe AK, whereas in mild and moderate patients, an increase in DC density was observed. This might also explain why DC density was lower than the result in the study by Cruzat et al.<sup>7</sup>

and not correlated with cyst density. Second, because IVCM can only provide a two-dimensional examination of a single plane at a time, three-dimensional DC might have not been analyzed precisely, particularly regarding the number of dendrites and the total DC length. The DC processes that were in a plane above or below the image plane were probably not quantified. This might explain why the results of DC dendrite numbers were not correlated with other parameters. Lastly, since our study was cross-sectional, the correlation between the number/density of cysts and the visual prognosis was not evaluated.

In conclusion, IVCM can provide a direct and reproducible method of observation of AK cysts and DCs in vivo. The cyst density and infiltration depth were correlated with disease severity. Patients with AK also showed an obvious increase in mature DCs in the central cornea, which might be used to monitor and adapt treatment, particularly regarding the inflammatory response.

## Acknowledgments

Supported by the Open Research Fund from Beijing Advanced Innovation Center for Big Data-Based Precision Medicine, Beijing Tongren Hospital, Beihang University & Capital Medical University (BHTR-KFJJ-202001) and the National Key R&D Program of China (No. 2017YFB1302703).

Disclosure: **Z. Wei**, None; **K. Cao**, None; **L. Wang**, None; **C. Baudouin**, None; **A. Labbé**, None; **Q. Liang**, None

## References

1. Kobayashi A, Yokogawa H, Higashide T, et al. Clinical significance of owl eye morphologic features by in vivo laser confocal microscopy in patients with cytomegalovirus corneal endothelitis. *Am J Ophthalmol*. 2012;153(3):445–453.
2. Nielsen SE, Ivarsen A, Hjortdal J. Increasing incidence of *Acanthamoeba* keratitis in a large tertiary ophthalmology department from year 1994 to 2018. *Acta Ophthalmol*. 2019, doi:10.1111/aos.14337.
3. Carnt N, Hoffman JJ MBBS, Verma S, et al. *Acanthamoeba* keratitis: confirmation of the UK outbreak and a prospective case-control study identifying contributing risk factors. *Br J Ophthalmol*. 2018;102(12):1621–1628.
4. Watt K, Swarbrick HA. Microbial keratitis in overnight orthokeratology: review of the first 50 cases. *Eye Contact Lens*. 2005;31(5):201–208.
5. Kremer I, Cohen EJ, Eagle RC, Jr., et al. Histopathologic evaluation of stromal inflammation in *Acanthamoeba* keratitis. *CLAO J*. 1994;20(1):45–48.
6. Sohn HJ, Seo GE, Lee JH, et al. Cytopathic change and inflammatory response of human corneal epithelial cells induced by *Acanthamoeba castellanii* trophozoites and cysts. *Korean J Parasitol*. 2019;57(3):217–223.
7. Cruzat A, Witkin D, Baniyasi N, et al. Inflammation and the nervous system: the connection in the cornea in patients with infectious keratitis. *Invest Ophthalmol Vis Sci*. 2011;52(8):5136–5143.
8. Harrison SM. Grading corneal ulcers. *Ann Ophthalmol*. 1975;7(4):537–542.
9. Acharya M, Farooqui JH, Jain S, et al. Pearls and paradigms in infective keratitis. *Rom J Ophthalmol*. 2019;63(2):119–127.
10. Huang P, Tepelus T, Vickers LA, et al. Quantitative analysis of depth, distribution, and density of cysts in *Acanthamoeba* keratitis using confocal microscopy. *Cornea*. 2017;36(8):927–932.
11. Rezaei Kanavi M, Naghshgar N, Javadi MA, et al. Various confocal scan features of cysts and trophozoites in cases with *Acanthamoeba* keratitis. *Eur J Ophthalmol*. 2012;22(Suppl 7):S46–S50.
12. Tu EY, Joslin CE, Sugar J, et al. The relative value of confocal microscopy and superficial corneal scrapings in the diagnosis of *Acanthamoeba* keratitis. *Cornea*. 2008;27(7):764–772.
13. Smedowski A, Tarnawska D, Orski M, et al. Cytoarchitecture of epithelial inflammatory infiltration indicates the aetiology of infectious keratitis. *Acta Ophthalmol*. 2017;95(4):405–413.
14. Zhivov A, Stave J, Vollmar B, et al. In vivo confocal microscopic evaluation of Langerhans cell density and distribution in the normal human corneal epithelium. *Graefes Arch Clin Exp Ophthalmol*. 2005;243(10):1056–1061.
15. Cavalcanti BM, Cruzat A, Sahin A, et al. In vivo confocal microscopy detects bilateral changes of corneal immune cells and nerves in unilateral herpes zoster ophthalmicus. *Ocul Surf*. 2018;16(1):101–111.
16. Kheirkhah A, Rahimi Darabad R, Cruzat A, et al. Corneal epithelial immune dendritic cell alterations in subtypes of dry eye disease: a pilot in vivo confocal microscopic study. *Invest Ophthalmol Vis Sci*. 2015;56:7179–7185.
17. Li S, Bian J, Wang Y, et al. Clinical features and serial changes of *Acanthamoeba* keratitis: an



- in vivo confocal microscopy study. *Eye (Lond)*. 2020;34(2):327–334.
18. Wang YE, Tepelus TC, Gui W, et al. Reduction of *Acanthamoeba* cyst density associated with treatment detected by in vivo confocal microscopy in *Acanthamoeba* keratitis. *Cornea*. 2019;38(4):463–468.
  19. Knickelbein JE, Kovarik J, Dhaliwal DK, et al. *Acanthamoeba* keratitis: a clinicopathologic case report and review of the literature. *Hum Pathol*. 2013;44(5):918–922.
  20. Clarke DW, Niederkorn JY. The immunobiology of *Acanthamoeba* keratitis. *Microbes Infect*. 2006; 8(5):1400–1405.
  21. Hanssens M, Jonckheere JFD, Meunynck CD. *Acanthamoeba* keratitis: a clinicopathological case report. *Int Ophthalmol*. 1985;7(3–4):203–213.
  22. Bancherau J, Steinman RM. Dendritic cells and the control of immunity. *Nature*. 1998;392(6673): 245–252.
  23. Ferrante A. Free-living amoebae: pathogenicity and immunity. *Parasite Immunol*. 1991;13(1):31–47.
  24. McClellan K, Howard K, Niederkorn JY, et al. Effect of steroids on *Acanthamoeba* cysts and trophozoites. *Invest Ophthalmol Vis Sci*. 2001; 42(12):2885–2893.
  25. Iovieno A, Gore DM, Carnt N, et al. *Acanthamoeba* sclerokeratitis: epidemiology, clinical features, and treatment outcomes. *Ophthalmology*. 2014;121(12):2340–2347.
  26. McClellan K, Howard K, Mayhew E, et al. Adaptive immune responses to *Acanthamoeba* cysts. *Exp Eye Res*. 2002;75(3):285–293.
  27. Chatterjee S, Agrawal D, Vemuganti GK. Granulomatous inflammation in *Acanthamoeba* sclerokeratitis. *Indian J Ophthalmol*. 2013;61(6):300–302.